

Outage Probability of UAV Communications in the Presence of Interference

Minsu Kim and Jemin Lee

Department of Information and Communication Engineering (ICE)
Daegu Gyeongbuk Institute of Science and Technology (DGIST), Korea
Email: ads5577@dgist.ac.kr, jmnlee@dgist.ac.kr

Abstract—Unlike terrestrial communications, unmanned aerial vehicle (UAV) communications have some advantages such as line-of-sight (LoS) environment and flexible mobility. However, the interference will be still inevitable. In this paper, we analyze the effect of the interference on the UAV communications by considering the LoS probability and different channel fadings for LoS and non-line-of-sight (NLoS) links, which are affected by the elevation angle of the communication link. We then derive a closed-form outage probability in the presence of an interfering node for all the possible scenarios and environments of main and interference links. After discussing the impacts of transmitting and interfering node parameters on the outage probability, we show the existence of the optimal height of the UAV that minimizes the outage probability. We also show the NLoS environment can be better than the LoS environment if the average received power of the interference is more dominant than that of the transmitting signal in UAV communications.

Index Terms—Unmanned aerial vehicle, interfering node, air-to-air channel, line-of-sight probability, outage probability

I. INTRODUCTION

As the unmanned aerial vehicle (UAV) technology develops, reliable UAV communications have become necessary. However, since UAV communications are different from conventional terrestrial communications, it is hard to apply the technology used in terrestrial communications to UAV communications [1]. Especially, unlike terrestrial communications, UAV communications can have line-of-sight (LoS) environments between a UAV and a ground device, and between UAVs. When the main link is in a LoS environment, the received main signal power will increase due to better channel fading and lower path loss exponent compared to a non-line-of-sight (NLoS) environment. It also means that in the presence of an interfering node, the interfering signal can be received with larger power as the interfering link can also be in a LoS environment [2].

UAV communications have been studied in the literature, mostly focused on the optimal positioning and trajectory of the UAV. The height of the UAV affects the communication performance in different ways. As the height increases, the

UAV forms the LoS link with higher probability, which is modeled by the LoS probability in [3], but the distance to the receiver at the ground increases as well. By considering this relation, the optimal height of the UAV in terms of the communication coverage in the air-to-ground (A2G) channel is presented in [4], and for the case of using an UAV as a relay, the optimal height and position of UAVs have also been presented in [5]. The work [6] jointly optimized UAV trajectory and power control to minimize the outage probability without considering the LoS probability. However, all of those works analyzed and optimized for the UAV communications in the absence of an interfering node. Since the interference is an inevitable factor in the current and future networks, the impact of the interference on the UAV communications needs to be investigated carefully.

Recently, the interference has been considered in some works for the optimal positioning and trajectory of the UAV. The optimal deployment of the UAV has been presented to maximize the communication coverage in [7], [8]. The user scheduling and UAV trajectory have been jointly optimized with maximizing the minimum average rate without considering the LoS probability in [9], and the UAV trajectory is also optimized jointly with device-UAV association and uplink power to minimize the total transmit power according to the number of update times in [10]. However, all of those prior works considered limited UAV communication scenarios or environments. Specifically, only the path loss is used for channels without fading in [8]–[10], or the fact that the LoS probability can be different according to the locations of the UAV was not considered in [7].

Therefore, in this paper, we analyze the effect of the interference on the UAV communications by considering both the LoS and NLoS links and channel fading. The probability of forming the LoS link is defined by the elevation angle between a UAV and a ground device, and the path loss exponent and the Rician factor are also determined differently by the elevation angle. The main contribution of this paper can be summarized as follows:

- we consider all the scenarios of main (i.e., from a transmitter to a receiver) and interference (i.e., from an interfering node to a receiver) links in UAV communications, which includes ground-to-air (G2A), ground-to-

This work was supported in part by the the National Research Foundation of Korea (NRF) grant funded by the Korea government (MSIP) (No. 2017R1C1B2009280) and the DGIST R&D Program of the Ministry of Science and ICT(17-ST-02).

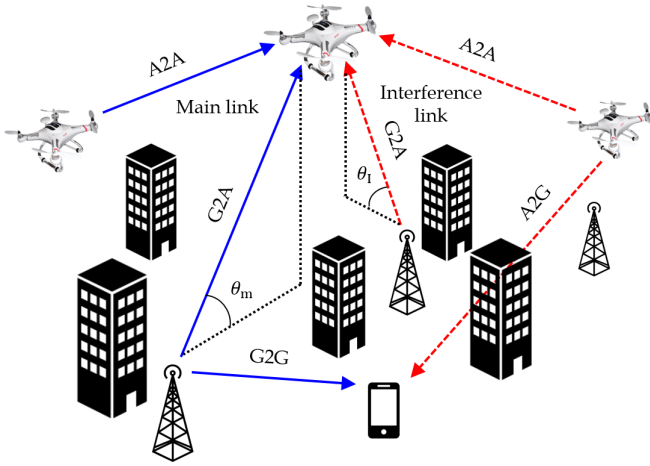


Fig. 1. System model when UAVs are the communication devices. There are four types of channels: ground-to-ground (G2G), ground-to-air (G2A), air-to-ground (A2G), and air-to-air (A2A) channels. The blue lines represent the main links and the red dotted lines represent the interference links, and θ_m and θ_I are the elevation angle of main link and interference link, respectively.

ground (G2G), A2G, and air-to-air (A2A) channels for the main and interference links;

- we derive a closed-form outage probability in the presence of interfering node for all the scenarios by considering the LoS probability and different channel fading for LoS and NLoS links; and
- we analyze how the heights of transmitting or interfering node and link distances affect the outage probability through numerical results.

II. SYSTEM MODEL

In this section, we describe the network model and the channel model for UAV communications.

A. Terrestrial & Aerial Network Models

We consider a UAV network, which has a UAV, a ground device (e.g., ground control station or base station), and an interfering node. In this network, there can be three types of communications: UAV to UAV, UAV to ground device (or ground device to UAV), and ground device to ground device. The interfering node can be either on the ground or in the air, and we consider one interfering node.¹

When a transmitter (Tx), located at (x_m, y_m, z_m) , communicates to a receiver (Rx), located at $(0, 0, z_o)$ in the presence of interfering node at (x_I, y_I, z_I) , signal-to-interference ratio (SIR) is given by

$$\gamma(\theta_m, \theta_I) = \frac{h_m \ell_m^{-\alpha_m(\theta_m)} P_m}{h_I \ell_I^{-\alpha_I(\theta_I)} P_I} = \frac{h_m \beta_m(\theta_m)}{h_I \beta_I(\theta_I)} \quad (1)$$

where $\beta_m(\theta_m)$ and $\beta_I(\theta_I)$ are respectively given by

$$\beta_m(\theta_m) = \ell_m^{-\alpha_m(\theta_m)} P_m, \quad \beta_I(\theta_I) = \ell_I^{-\alpha_I(\theta_I)} P_I. \quad (2)$$

¹Note that when the multiple interfering nodes are considered, the communication performance such as the outage probability has the similar trend as only dominant interfering node is considered and it is generally determined by the dominant interfering node at the low outage region [11].

Here, h_m and h_I are the fading gains of the main link (i.e., the channel between Tx and Rx) and the interference link (i.e., the channel between interfering node and Rx), respectively; $\ell_m = \sqrt{x_m^2 + y_m^2 + (z_m - z_o)^2}$ and $\ell_I = \sqrt{x_I^2 + y_I^2 + (z_I - z_o)^2}$ are the distances of main link and interference link, respectively; P_m and P_I are the transmission power of the transmitter and the interfering node, respectively; and $\alpha_m(\theta_m)$ and $\alpha_I(\theta_I)$ are the path loss exponents of main link and interference link, respectively. In (1), most parameters are determined by θ_m and θ_I , which are the elevation angles between Tx and Rx and between Rx and the interfering node, respectively, which are given by

$$\theta_i = \arctan \left(\frac{d_i^{(V)}}{d_i^{(H)}} \right), \quad \forall i = \{m, I\} \quad (3)$$

where $d_i^{(H)} = \sqrt{x_i^2 + y_i^2}$ is the horizontal distance and $d_i^{(V)} = \sqrt{(z_i - z_o)^2}$ is the vertical distance of the main link ($i = m$) or the interference link ($i = I$).

B. Channel Model

As shown in Fig. 1, there are three types of the channels in the UAV networks: the *A2G channel* (from UAV to a ground device), the *A2A channel* (from UAV to UAV), and the *G2G channel* (from a ground device to a ground device). The G2G channel is the same channel of a terrestrial network, which is generally modeled as NLoS environments with Rayleigh fading in urban area. The G2A channel and the A2G channel have the same characteristics. Hence, we describe characteristics of the A2G and A2A channels in this subsection.

The A2G and A2A channels can have LoS or NLoS environments depending on the height of the UAV and its surrounding environments such as buildings. The elevation angle θ_i (θ_m or θ_I) is considered for the A2G (or G2A) channel, while ignored for G2G or A2A channel and assumed to be $\theta_i = 0$ or $\frac{\pi}{2}$ for those two cases. In the following, we first describe the channel components, affected by θ_i , and then provide the models for A2G and A2A channels.

1) *Components affected by elevation angle θ_i* : The elevation angle θ_i affects the probability of forming LoS, the path loss exponent, and the Rician factor as described below.

- The *LoS probability* is given by [3]

$$p_L(\theta_i) = \frac{1}{1 + a_1 \exp\{-b_1(\theta_i - a_1)\}} \quad (4)$$

where a_1 and b_1 are environment parameters, determined by the building density and height.

- The *path loss exponent* is determined by θ_i as [5]

$$\alpha(\theta_i) = a_2 p_L(\theta_i) + b_2 \quad (5)$$

where $a_2 = \frac{\alpha(\frac{\pi}{2}) - \alpha(0)}{p_L(\frac{\pi}{2}) - p_L(0)} \approx \alpha(\frac{\pi}{2}) - \alpha(0)$ and $b_2 = \alpha(0) - a_2 p_L(0) \approx \alpha(0)$.

- The *Rician factor* is determined by θ_i as [5]

$$K(\theta_i) = a_3 \exp(b_3 \theta_i) \quad (6)$$

where $a_3 = K(0)$ and $b_3 = \frac{2}{\pi} \ln \left(\frac{K(\frac{\pi}{2})}{K(0)} \right)$.

$$p_o^{(L,L)}(\Theta, \mathcal{D}) = 1 - Q \left(\sqrt{\frac{2K_m(\theta_m)\beta_m(\theta_m)}{\beta_m(\theta_m) + \gamma_t\beta_I(\theta_I)}}, \sqrt{\frac{2\gamma_t K_I(\theta_I)\beta_I(\theta_I)}{\beta_m(\theta_m) + \gamma_t\beta_I(\theta_I)}} \right) + \frac{\gamma_t\beta_I(\theta_I)}{\beta_m(\theta_m) + \gamma_t\beta_I(\theta_I)} \\ \times \exp \left(-\frac{K_m(\theta_m)\beta_m(\theta_m) + \gamma_t K_I(\theta_I)\beta_I(\theta_I)}{\beta_m(\theta_m) + \gamma_t\beta_I(\theta_I)} \right) I_0 \left(\frac{2\beta_m(\theta_m)}{\beta_m(\theta_m) + \gamma_t\beta_I(\theta_I)} \sqrt{\frac{\gamma_t K_m(\theta_m) K_I(\theta_I)\beta_I(\theta_I)}{\beta_m(\theta_m)}} \right) \quad (13)$$

Note that from (4)-(6), we can see that $p_L(\theta_i)$ and $K(\theta_i)$ are increasing functions of θ_i and $\alpha(\theta_i)$ is a decreasing function of θ_i , so the received power increases when θ_i increases.

2) *Air-to-Ground (A2G) channel*: When the main link and the interference link are both A2G channels, h_m and h_I can be in either LoS or NLoS environments. We consider that the channel fading is Rician fading for LoS environments and Rayleigh fading for NLoS environments. Therefore, the distribution of the channel fading, $h_i, i \in \{m, I\}$, is given by

$$f_{h_i}(h) = \begin{cases} f_L(h) & \text{for LoS case} \\ f_N(h) & \text{for NLoS case} \end{cases} \quad (7)$$

where $f_L(h)$ and $f_N(h)$ are noncentral Chi-squared and exponential distribution, respectively, and given by

$$f_L(h) = \frac{1 + K(\theta_i)}{\overline{H}_L} \exp \left(-K(\theta_i) - \frac{1 + K(\theta_i)}{\overline{H}_L} h \right) \\ \times I_0 \left(2\sqrt{\frac{K(\theta_i)(1 + K(\theta_i))}{\overline{H}_L}} h \right) \\ = \frac{1}{2} \exp \left(-K(\theta_i) - \frac{h}{2} \right) I_0 \left(\sqrt{2K(\theta_i)h} \right) \quad (8)$$

$$f_N(h) = \frac{1}{\overline{H}_N} \exp \left(-\frac{h}{\overline{H}_N} \right) = \exp(-h). \quad (9)$$

Here, $I_0(\cdot)$ is the modified Bessel function of the first kind with order zero, and $\overline{H}_L = 2 + 2K(\theta_i)$ and $\overline{H}_N = 1$ are the means of LoS and NLoS channel fading gain, respectively.

3) *Air-to-Air (A2A) channel*: In A2A channel, the channel will be in LoS environments and $\theta_i = \frac{\pi}{2}$, so the distribution of the channel fading, $h_i, i \in \{m, I\}$, is given by

$$f_{h_i}(h) = \frac{1}{2} \exp \left(-K_o - \frac{h}{2} \right) I_0 \left(\sqrt{2K_o h} \right) \quad (10)$$

where $K_o = K(\frac{\pi}{2})$. Unlike the A2G channel, the Rician factor K_o and the path loss exponent α of A2A channel are not affected by θ_i [12].

III. OUTAGE PROBABILITY ANALYSIS

In this section, we analyze the outage probability by considering various environments of main and interference links. For given the elevation angle set $\Theta = (\theta_m, \theta_I)$ and the link distance set $\mathcal{D} = (\ell_m, \ell_I)$ of main and interference links, the outage probability is defined as

$$p_o(\Theta, \mathcal{D}) = \mathbb{P}[\gamma(\theta_m, \theta_I) < \gamma_t] \quad (11)$$

where γ_t is the target SIR, which can be defined by $\gamma_t = \frac{R_t}{2\frac{R_t}{W}} - 1$ for the target rate R_t and the bandwidth W [13]. We

consider the interference limited environment, and the derived outage probabilities are given in the following theorem.

Theorem 1: For given $\Theta = (\theta_m, \theta_I)$ and $\mathcal{D} = (\ell_m, \ell_I)$, the outage probability $p_o(\Theta, \mathcal{D})$ can be presented as

$$p_o(\Theta, \mathcal{D}) = p_L(\theta_m)p_L(\theta_I)p_o^{(L,L)}(\Theta, \mathcal{D}) \\ + p_L(\theta_m)(1 - p_L(\theta_I))p_o^{(L,N)}(\Theta, \mathcal{D}) \\ + (1 - p_L(\theta_m))p_L(\theta_I)p_o^{(N,L)}(\Theta, \mathcal{D}) \\ + (1 - p_L(\theta_m))(1 - p_L(\theta_I))p_o^{(N,N)}(\Theta, \mathcal{D}) \quad (12)$$

where $p_o^{(e_m, e_I)}(\Theta, \mathcal{D})$ is the outage probability with the environment of the main link e_m and that of the interference link e_I . The environment e_i can be either LoS (i.e., $e_i = L$) or NLoS (i.e., $e_i = N$), and $p_o^{(e_m, e_I)}(\Theta, \mathcal{D})$ for four cases of (e_m, e_I) are given as follows:

1) *Case 1* ($e_m = L$ and $e_I = L$): $p_o^{(L,L)}(\Theta, \mathcal{D})$ is given by (13).

2) *Case 2* ($e_m = L$ and $e_I = N$): $p_o^{(L,N)}(\Theta, \mathcal{D})$ is given by

$$p_o^{(L,N)}(\Theta, \mathcal{D}) = \frac{\gamma_t\beta_I(\theta_I)}{2\beta_m(\theta_m) + \gamma_t\beta_I(\theta_I)} \\ \times \exp \left(-\frac{2K_m(\theta_m)\beta_m(\theta_m)}{2\beta_m(\theta_m) + \gamma_t\beta_I(\theta_I)} \right). \quad (14)$$

3) *Case 3* ($e_m = N$ and $e_I = L$): $p_o^{(N,L)}(\Theta, \mathcal{D})$ is given by

$$p_o^{(N,L)}(\Theta, \mathcal{D}) = 1 - \frac{\beta_m(\theta_m)}{2\gamma_t\beta_I(\theta_I) + \beta_m(\theta_m)} \\ \times \exp \left(-\frac{2\gamma_t K_I(\theta_I)\beta_I(\theta_I)}{2\gamma_t\beta_I(\theta_I) + \beta_m(\theta_m)} \right). \quad (15)$$

4) *Case 4* ($e_m = N$ and $e_I = N$): $p_o^{(N,N)}(\Theta, \mathcal{D})$ is given by

$$p_o^{(N,N)}(\Theta, \mathcal{D}) = \frac{\gamma_t\beta_I(\theta_I)}{\beta_m(\theta_m) + \gamma_t\beta_I(\theta_I)}. \quad (16)$$

Proof: The outage probability is obtained as (12) using the law of total probability. We derive $p_o^{(e_m, e_I)}(\Theta, \mathcal{D})$ for the above four cases as follows. For *Case 1*, $K_m(\theta_m) \neq 0$ and $K_I(\theta_I) \neq 0$ as both main and interference links are in LoS environments, and $p_o^{(L,L)}(\Theta, \mathcal{D})$ can be obtained using (8) as

$$p_o^{(L,L)}(\Theta, \mathcal{D}) = \int_0^\infty \int_0^\infty \frac{\gamma_t\beta_I(\theta_I)g}{\beta_m(\theta_m)} f_{h_m}(h) dh f_{h_I}(g) dg \\ \stackrel{(a)}{=} 1 - \frac{1}{2} \int_0^\infty Q \left(\sqrt{2K_m(\theta_m)}, \sqrt{\frac{\gamma_t\beta_I(\theta_I)g}{\beta_m(\theta_m)}} \right) \\ \times \exp \left(-K_I(\theta_I) - \frac{g}{2} \right) I_0 \left(\sqrt{2K_I(\theta_I)g} \right) dg \quad (17)$$

where $Q(a, b)$ is the first-order Marcum Q-function. In (17),

(a) is from the cumulative distribution function (CDF) of the noncentral Chi-squared distribution, and the integral term can be presented as

$$\begin{aligned} & \int_0^\infty \exp(-c^2x) I_0(d\sqrt{2x}) Q(e, f\sqrt{2x}) dx \\ &= \frac{1}{c^2} \left\{ \exp\left(\frac{d^2}{2c^2}\right) Q\left(\frac{ce}{\sqrt{c^2+f^2}}, \frac{df}{c\sqrt{c^2+f^2}}\right) \right. \\ & \quad \left. - \frac{f^2}{c^2+f^2} \exp\left(\frac{d^2-c^2e^2}{2(c^2+f^2)}\right) I_0\left(\frac{def}{c^2+f^2}\right) \right\} \quad (18) \end{aligned}$$

where $c = \sqrt{0.5}$, $d = \sqrt{K_I(\theta_I)}$, $e = \sqrt{2K_m(\theta_m)}$, and $f = \sqrt{\frac{\gamma_t \beta_I(\theta_I)}{2\beta_m(\theta_m)}}$ from [14, eq. (46)]. By using (18) in (17), $p_o^{(L,L)}(\Theta, \mathcal{D})$ is presented as (13).

In Case 2, $K_m(\theta_m) \neq 0$ and $K_I(\theta_I) = 0$ as the interference link is in NLoS environment, and $p_o^{(L,N)}(\Theta, \mathcal{D})$ is obtained using (8) and (9) as

$$\begin{aligned} p_o^{(L,N)}(\Theta, \mathcal{D}) &= \int_0^\infty \int_0^{\frac{\gamma_t \beta_I(\theta_I)g}{\beta_m(\theta_m)}} f_{h_m}(h) dh f_{h_I}(g) dg \\ &= 1 - \int_0^\infty Q\left(\sqrt{2K_m(\theta_m)}, \sqrt{\frac{\gamma_t \beta_I(\theta_I)g}{\beta_m(\theta_m)}}\right) \exp(-g) dg. \quad (19) \end{aligned}$$

In (19), the integral term can be presented as

$$\begin{aligned} & \int_0^\infty \exp(-c^2x) Q(e, f\sqrt{2x}) dx \\ &= \frac{1}{c^2} \left\{ 1 - \frac{f^2}{c^2+f^2} \exp\left(-\frac{c^2e^2}{2(c^2+f^2)}\right) \right\} \quad (20) \end{aligned}$$

where $c=1$, $e = \sqrt{2K_m(\theta_m)}$, and $f = \sqrt{\frac{\gamma_t \beta_I(\theta_I)}{2\beta_m(\theta_m)}}$ from [14, eq. (40)]. By using (20) in (19), $p_o^{(L,N)}(\Theta, \mathcal{D})$ is presented as (14).

In Case 3, $K_m(\theta_m) = 0$ and $K_I(\theta_I) \neq 0$ as the main link is in NLoS environment, and $p_o^{(N,L)}(\Theta, \mathcal{D})$ is given by

$$\begin{aligned} p_o^{(N,L)}(\Theta, \mathcal{D}) &= \int_0^\infty \int_0^{\frac{\gamma_t \beta_I(\theta_I)g}{\beta_m(\theta_m)}} f_{h_m}(h) dh f_{h_I}(g) dg \\ &\stackrel{(a)}{=} 1 - \frac{1}{2} \int_0^\infty \exp\left(-\frac{\gamma_t \beta_I(\theta_I)g}{\beta_m(\theta_m)}\right) \\ & \quad \times \exp\left(-K_I(\theta_I) - \frac{g}{2}\right) I_0\left(\sqrt{2K_I(\theta_I)g}\right) dg \quad (21) \end{aligned}$$

In (21), (a) is from the CDF of the exponential distribution and the integral term can be presented as

$$\int_0^\infty \exp(-c^2x) I_0(d\sqrt{2x}) dx = \frac{1}{c^2} \exp\left(\frac{d^2}{2c^2}\right) \quad (22)$$

where $c = \sqrt{\frac{1}{2} + \frac{\gamma_t \beta_I(\theta_I)}{\beta_m(\theta_m)}}$ and $d = \sqrt{K_I(\theta_I)}$ from [14, eq. (9)]. By using (22) in (21), $p_o^{(N,L)}(\Theta, \mathcal{D})$ is presented as (15).

In Case 4, $K_m(\theta_m) = 0$ and $K_I(\theta_I) = 0$ as the main and the interference links are both in NLoS environments, and $p_o^{(N,N)}(\Theta, \mathcal{D})$ is given by

$$p_o^{(N,N)}(\Theta, \mathcal{D}) = \int_0^\infty \int_0^{\frac{\gamma_t \beta_I(\theta_I)g}{\beta_m(\theta_m)}} f_{h_m}(h) dh f_{h_I}(g) dg$$

TABLE I
 $\Theta = (\theta_m, \theta_I)$ IN OUTAGE PROBABILITY

Interferer				
Main		A2A	A2G (G2A)	G2G
A2A		$(\frac{\pi}{2}, \frac{\pi}{2})$	$(\frac{\pi}{2}, \theta_I)$	
A2G (G2A)		$(\theta_m, \frac{\pi}{2})$	(θ_m, θ_I)	$(\theta_m, 0)$
G2G			$(0, \theta_I)$	$(0, 0)$

$$= 1 - \int_0^\infty \exp\left(-\frac{\gamma_t \beta_I(\theta_I)g}{\beta_m(\theta_m)} - g\right) dg. \quad (23)$$

By simple calculation in (23), $p_o^{(N,N)}(\Theta, \mathcal{D})$ is obtained as (16). ■

From Theorem 1, we can also obtain the outage probability as for different scenarios of UAV communications by changing the values of (Θ, \mathcal{D}) . Specifically, according to whether the main link or interference link is A2A, A2G (G2A), or G2G channel, we can set (Θ, \mathcal{D}) in (12) as the values in Table I to obtain the outage probability in certain scenarios.

In Theorem 1, we can readily know $p_o^{(L,N)}(\Theta, \mathcal{D})$ (Case 2) cannot be higher than $p_o^{(N,L)}(\Theta, \mathcal{D})$ (Case 3) as Case 2 has stronger main link and weaker interference link than Case 3. However, it is not clear whether the outage probability with LoS environments for both main and interference links (Case 1) can be lower or higher than that with NLoS environments for both main and interference links (Case 4). Hence, we compare $p_o^{(L,L)}(\Theta, \mathcal{D})$ and $p_o^{(N,N)}(\Theta, \mathcal{D})$, and obtain the following results in Corollary 1.

Corollary 1: According to the ratio of the average received signal power of main and interference links, i.e., $\frac{\beta_m(\theta_m)}{\beta_I(\theta_I)}$, the relation between $p_o^{(L,L)}(\Theta, \mathcal{D})$ and $p_o^{(N,N)}(\Theta, \mathcal{D})$ is changed as

$$\begin{cases} p_o^{(L,L)}(\Theta, \mathcal{D}) > p_o^{(N,N)}(\Theta, \mathcal{D}), & \text{if } \frac{\beta_m(\theta_m)}{\beta_I(\theta_I)} < v' \\ p_o^{(L,L)}(\Theta, \mathcal{D}) < p_o^{(N,N)}(\Theta, \mathcal{D}), & \text{if } \frac{\beta_m(\theta_m)}{\beta_I(\theta_I)} > v' \\ p_o^{(L,L)}(\Theta, \mathcal{D}) = p_o^{(N,N)}(\Theta, \mathcal{D}), & \text{if } \frac{\beta_m(\theta_m)}{\beta_I(\theta_I)} = 0, \infty, \text{ or } v' \end{cases} \quad (24)$$

where v' ($0 < v' < \infty$) is the value of $\frac{\beta_m(\theta_m)}{\beta_I(\theta_I)}$ that makes $p_o^{(L,L)}(\Theta, \mathcal{D}) = p_o^{(N,N)}(\Theta, \mathcal{D})$.

Proof: For convenience, we introduce $v = \frac{\beta_m(\theta_m)}{\beta_I(\theta_I)}$, and define $A(v)$ and $B(v)$ as

$$A(v) = \sqrt{\frac{2K_m(\theta_m)v}{v + \gamma_t}}, \quad B(v) = \sqrt{\frac{2\gamma_t K_I(\theta_I)}{v + \gamma_t}}. \quad (25)$$

By using (25), $p_o^{(L,L)}(\Theta, \mathcal{D})$ in (13) and $p_o^{(N,N)}(\Theta, \mathcal{D})$ in (16) can rewrite as functions of v as

$$\begin{aligned} p_o^{(L,L)}(v) &= 1 - Q(A(v), B(v)) + \frac{\gamma_t}{v + \gamma_t} \\ & \quad \times \exp\left(-\frac{A(v)^2 + B(v)^2}{2}\right) I_0(A(v)B(v)) \\ p_o^{(N,N)}(v) &= \frac{\gamma_t}{v + \gamma_t}. \quad (26) \end{aligned}$$

From (26), we obtain the first derivatives of $p_o^{(L,L)}(v)$ and $p_o^{(N,N)}(v)$ according to v , respectively, as

$$\begin{aligned} \frac{\partial p_o^{(L,L)}(v)}{\partial v} &= \left(p_o^{(N,N)}(v) - 1 \right) \exp\left(-\frac{A(v)^2 + B(v)^2}{2}\right) B(v) \\ &\times \left\{ I_1(A(v)B(v)) \frac{\partial A(v)}{\partial v} - I_0(A(v)B(v)) \frac{\partial B(v)}{\partial v} \right\} \\ &+ p_o^{(N,N)}(v) \exp\left(-\frac{A(v)^2 + B(v)^2}{2}\right) A(v) \\ &\times \left\{ I_1(A(v)B(v)) \frac{\partial B(v)}{\partial v} - I_0(A(v)B(v)) \frac{\partial A(v)}{\partial v} \right\} \\ &+ \frac{\partial p_o^{(N,N)}(v)}{\partial v} \exp\left(-\frac{A(v)^2 + B(v)^2}{2}\right) I_0(A(v)B(v)) < 0 \end{aligned} \quad (27)$$

$$\frac{\partial p_o^{(N,N)}(v)}{\partial v} = -\frac{\gamma_t}{(v + \gamma_t)^2} < 0. \quad (28)$$

In (27) and (28), the inequalities are obtained since $\exp(v) \geq 1$, $I_0(v) \geq 1$, $A(v) \geq 0$, $B(v) \geq 0$, $I_1(v) \geq 0$, $\frac{\partial A(v)}{\partial v} \geq 0$, $\frac{\partial B(v)}{\partial v} \leq 0$, and $0 \leq p_o^{(N,N)}(v) \leq 1$. Hence, $p_o^{(L,L)}(v)$ and $p_o^{(N,N)}(v)$ are monotonically decreasing functions of v .

If $v = 0$, from (28) and (27), we have

$$\frac{\partial p_o^{(N,N)}(0)}{\partial v} < \frac{\partial p_o^{(L,L)}(0)}{\partial v} \quad (29)$$

since $\frac{\partial p_o^{(N,N)}(0)}{\partial v} = -\frac{1}{\gamma_t}$, $\frac{\partial p_o^{(L,L)}(0)}{\partial v} = \frac{\partial p_o^{(N,N)}(0)}{\partial v} \exp\left(-\frac{B(0)^2}{2}\right)$, and $p_o^{(N,N)}(0) = p_o^{(L,L)}(0) = 1$. Hence, for small ϵ , we have

$$p_o^{(N,N)}(\epsilon) < p_o^{(L,L)}(\epsilon). \quad (30)$$

If v approaches ∞ , $B(v) \rightarrow 0$, $\lim_{v \rightarrow \infty} p_o^{(L,L)}(v) = \lim_{v \rightarrow \infty} p_o^{(N,N)}(v) = 0$, and from (28) and (27), we have

$$\begin{aligned} \frac{\partial p_o^{(N,N)}(v)}{\partial v} &\rightarrow -\frac{\gamma_t}{(v + \gamma_t)^2}, \\ \frac{\partial p_o^{(L,L)}(v)}{\partial v} &\rightarrow \frac{\partial p_o^{(N,N)}(v)}{\partial v} \exp\left(-\frac{A(v)^2}{2}\right). \end{aligned} \quad (31)$$

From (31), we can see that for large $v_o \gg 1$, $\frac{\partial p_o^{(L,L)}(v_o)}{\partial v} > \frac{\partial p_o^{(N,N)}(v_o)}{\partial v}$, and we have

$$p_o^{(L,L)}(v_o) < p_o^{(N,N)}(v_o) \quad (32)$$

Therefore, from (30), (32), and the fact that $p_o^{(L,L)}(v)$ and $p_o^{(N,N)}(v)$ are both monotonically decreasing functions, we can know that there exists unique point v' in $0 < v' < \infty$ that makes $p_o^{(L,L)}(v') = p_o^{(N,N)}(v')$. Therefore, we obtain (24). ■

From Corollary 1, when the main and interference links are in the same environment, NLoS environment can be more preferred if the average received power of interference is much larger than that of transmitting signal (i.e., small $\frac{\beta_m(\theta_m)}{\beta_i(\theta_i)}$), but for the opposite case (i.e., large $\frac{\beta_m(\theta_m)}{\beta_i(\theta_i)}$), LoS environment can be better in terms of outage probability.

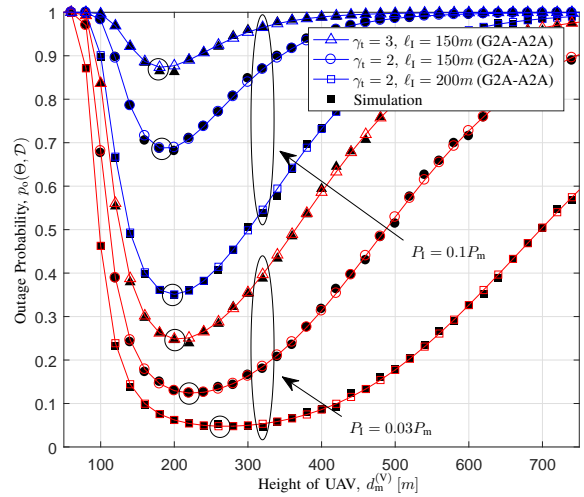


Fig. 2. Outage probability $p_o(\Theta, \mathcal{D})$ as a function of height $d_m^{(V)}$ with $d_m^{(H)} = 100m$ for different values of γ_t , ℓ_1 , and P_i . The circle means the optimal height with the lowest outage probability.

IV. NUMERICAL RESULTS

In this section, we present the effects of height, parameters, and channel state on the outage probability. Unless otherwise specified, the values of simulation parameters are $a_1=12.08$, $b_1=0.11$, $\alpha_0=3.5$, $\alpha_{\frac{\pi}{2}}=2$, $k_0=1$, $k_{\frac{\pi}{2}}=15$, and $P_m=10^{-8}W$.

Fig. 2 presents the outage probability $p_o(\Theta, \mathcal{D})$ as a function of height $d_m^{(V)}$ with $d_m^{(H)} = 100m$ for different values of γ_t , ℓ_1 , and P_i . The main link is the G2A channel of which the horizontal distance is fixed as 100m and the vertical distance, i.e., the height of UAV, only increases. To focus on the impact of the UAV height on $p_o(\Theta, \mathcal{D})$, the environment of interference link is set to be the same over different height of UAV such as the A2A channel with fixed link distance ℓ_1 . In Fig. 2, it is shown that the analytic results closely match with the simulation results.

From Fig. 2, we can see that the outage probability first decreases as the height increases up to a certain value of the height, and then increases. This is because the LoS probability of main link increases as the height increases. When the height of UAV is small, as the height increases, the increasing probability of forming LoS main link is more dominant than the increasing main link distance on the outage probability. However, for large height, the LoS probability does not change that much with the height while the link distance becomes longer, so the outage probability increases. We can also see that the optimal height that minimizes $p_o(\Theta, \mathcal{D})$ increases as the target SIR γ_t or the power of interference link P_i decreases or the distance of interference link ℓ_1 increases. From this, we can know that the optimal height increases as the impact of interference link on the communication reduces.

Fig. 3 presents the outage probability $p_o(\Theta, \mathcal{D})$ as a function of $d_1^{(H)}$ with $P_i = P_m$ and $\gamma_t = 2$ for different values of $d_1^{(V)}$ and channel state of main link. To focus on the impact of the horizontal and vertical distance of interference link, the main link is set as the A2A or the G2G channel with a fixed link distance 100m. The interference link is

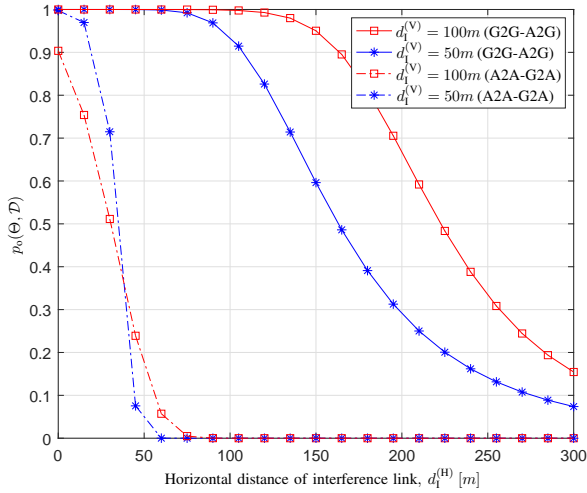


Fig. 3. Outage probability $p_o(\Theta, \mathcal{D})$ as a function of $d_1^{(H)}$ with $P_1 = P_m$ and $\gamma_t = 2$ for different values of $d_1^{(V)}$ and channel state of main link.

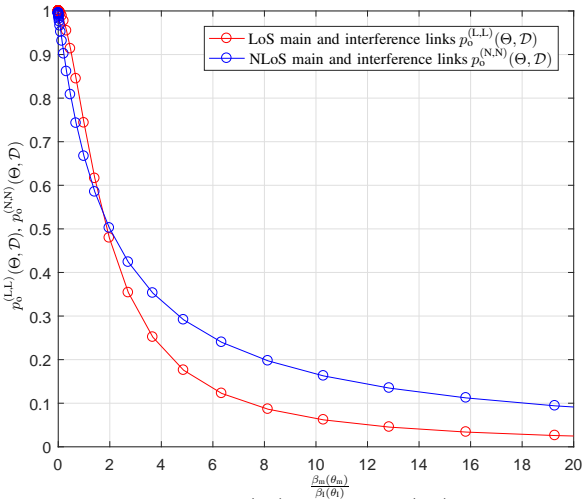


Fig. 4. Outage probabilities $p_o^{(L,L)}(\Theta, \mathcal{D})$ and $p_o^{(N,N)}(\Theta, \mathcal{D})$ as a function of $\frac{\beta_m(\theta_m)}{\beta_1(\theta_1)}$ with $d_m^{(H)} = 100m$, $d_1^{(V)} = d_m^{(V)} = 70m$, and $\gamma_t = 2$.

the A2G or the G2A channel. From this figure, we can see that generally, longer horizontal distance of interference link (i.e., larger $d_1^{(H)}$) results in lower outage probability. On the other hand, longer vertical distance of interference link (i.e., larger $d_1^{(V)}$) does not always result in lower outage probability. Specifically, when the main link is the A2A channel, the outage probability can be smaller with $d_1^{(V)} = 50m$ than with $d_1^{(V)} = 100m$. This is because, as $d_1^{(H)}$ increases, the LoS probability of interference link with $d_1^{(V)} = 50m$ decreases faster than that with $d_1^{(V)} = 100m$.

Fig. 4 presents the outage probabilities $p_o^{(L,L)}(\Theta, \mathcal{D})$ and $p_o^{(N,N)}(\Theta, \mathcal{D})$ as a function of $\frac{\beta_m(\theta_m)}{\beta_1(\theta_1)}$ with $d_m^{(H)} = 100m$, $d_1^{(V)} = d_m^{(V)} = 70m$, and $\gamma_t = 2$. From this figure, we can confirm that both outage probabilities are monotonic decreasing functions with $\frac{\beta_m(\theta_m)}{\beta_1(\theta_1)}$. In addition, there exists a cross point of those probabilities at around $\frac{\beta_m(\theta_m)}{\beta_1(\theta_1)} = 1.7$. For smaller $\frac{\beta_m(\theta_m)}{\beta_1(\theta_1)} < 1.7$, $p_o^{(L,L)}(\Theta, \mathcal{D})$ is greater than $p_o^{(N,N)}(\Theta, \mathcal{D})$, but it becomes opposite for larger $\frac{\beta_m(\theta_m)}{\beta_1(\theta_1)} > 1.7$. This verifies the

results in Corollary 1.

V. CONCLUSION

This paper analyzes the impact of the interfering node for reliable UAV communications. After characterizing the channel model affected by the elevation angle of the communication link, we derive the outage probability in a closed form for all possible scenarios of main and interference links. Furthermore, we show the effects of the transmission power, the horizontal and vertical link distances, and the communication scenarios of main and interference links. Specifically, we show the existence of the optimal height of the UAV for different scenarios, which increases as the power of interfering node increases or the interference link distance decreases. We also analytically prove that NLoS environment can be better than LoS environment if the average received power of interference is much larger than that of transmitting signal. The outcomes of our work can provide insights on the optimal deployment of UAV in the presence of interfering node.

REFERENCES

- [1] Y. Zeng, R. Zhang, and T. J. Lim, "Wireless communications with unmanned aerial vehicles: opportunities and challenges," *IEEE Commun. Mag.*, vol. 54, no. 5, pp. 36–42, May 2016.
- [2] H. Cho, C. Liu, J. Lee, T. Noh, and T. Q. S. Quek, "Impact of elevated base stations on the ultra-dense networks," *IEEE Commun. Lett.*, vol. 22, no. 6, pp. 1268–1271, Jun. 2018.
- [3] P. Series, "Propagation data and prediction methods required for the design of terrestrial broadband radio access systems operating in a frequency range from 3 to 60 GHz," *Recommendation ITU-R*, pp. 1410–1415, 2013.
- [4] A. Al-Hourani, S. Kandeepan, and S. Lardner, "Optimal LAP altitude for maximum coverage," *IEEE Wireless Commun. Lett.*, vol. 3, no. 6, pp. 569–572, Dec. 2014.
- [5] M. M. Azari, F. Rosas, K. C. Chen, and S. Pollin, "Ultra reliable UAV communication using altitude and cooperation diversity," *IEEE Trans. Commun.*, vol. 66, no. 1, pp. 330–344, Jan. 2018.
- [6] S. Zhang, H. Zhang, Q. He, K. Bian, and L. Song, "Joint trajectory and power optimization for UAV relay networks," *IEEE Commun. Lett.*, vol. 22, no. 1, pp. 161–164, Jan. 2018.
- [7] V. V. Chetnur and H. S. Dhillon, "Downlink coverage analysis for a finite 3-D wireless network of unmanned aerial vehicles," *IEEE Trans. Commun.*, vol. 65, no. 10, pp. 4543–4558, Oct. 2017.
- [8] M. Mozaffari, W. Saad, M. Bennis, and M. Debbah, "Unmanned aerial vehicle with underlaid device-to-device communications: Performance and tradeoffs," *IEEE Trans. Wireless Commun.*, vol. 15, no. 6, pp. 3949–3963, Jun. 2016.
- [9] Q. Wu, Y. Zeng, and R. Zhang, "Joint trajectory and communication design for multi-UAV enabled wireless networks," *IEEE Trans. Wireless Commun.*, vol. 17, no. 3, pp. 2109–2121, Mar. 2018.
- [10] M. Mozaffari, W. Saad, M. Bennis, and M. Debbah, "Mobile unmanned aerial vehicles (UAVs) for energy-efficient Internet of Things communications," *IEEE Trans. Wireless Commun.*, vol. 16, no. 11, pp. 7574–7589, Nov. 2017.
- [11] V. Mordachev and S. Loyka, "On node density-outage probability tradeoff in wireless networks," *IEEE J. Sel. Areas Commun.*, vol. 27, no. 7, pp. 1120–1131, Sep. 2009.
- [12] N. Goddemeier and C. Wietfeld, "Investigation of air-to-air channel characteristics and a UAV specific extension to the Rice model," in *Proc. IEEE Global Commun. Conf. Workshops. (GC Wkshps)*, San Diego, CA, Dec. 2015, pp. 1–5.
- [13] W. Limpakom, Y. D. Yao, and H. Man, "Outage probability analysis of wireless relay and cooperative networks in Rician fading channels with different K-factors," in *Proc. IEEE Veh. Technol. Conf. (VTC)*, Barcelona, Spain, Apr. 2009, pp. 1–5.
- [14] A. H. Nuttall, "Some integrals involving the Q-function," Naval Underwater Systems Center (NUSC) Technical Report 4297, Tech. Rep., Apr. 1972.